Optimization of Crystallization Dynamics in Wide-Bandgap Bromine-Iodine Perovskite Films for High-Performance Perovskite-Organic Tandem Solar Cells

Zonglong Song[#a], *Jiangfeng Wang*[#a], *Yuqi Bao*[a], *Jie Zeng*[a], *Deng Wang*[a], *Jiang He*[a], *Peide Zhu*[a], *Bo Jiang*[a], *Zhixin Liu*[a], *Siru He*[a], *Yanna Hou*[g], *Ziyang Hu*[g], *Chen Xie*[h], *Yongsheng Chen*[f], *Yongsheng Liu*[ef]*, *Xingzhu Wang*[abcd]*, *Baomin Xu*[ab]*

[a]Department of Materials Science and Engineering, Southern University of Science and Technology, Shenzhen, 518055, China.

[b]Department of Materials Science and Engineering, Shenzhen Engineering Research and Development Center for Flexible Solar Cells, and SUSTech Energy Institute for Carbon Neutrality, Southern University of Science and Technology, Shenzhen, 518055, China, xubm@sustech.edu.cn.

[c]Shenzhen Putai Technology Co., Ltd, Shenzhen, 518110, China, wangxz@sustech.edu.cn.

[d]School of Electrical Engineering, University of South China, Hengyang, 421001, China.

[e]The Centre of Nanoscale Science and Technology and Key Laboratory of Functional Polymer Materials, Institute of Polymer Chemistry, College of Chemistry and Renewable Energy Conversion and Storage Center (RECAST), Nankai University, Tianjin, 300071, China.

[f]The Centre of Nanoscale Science and Technology and Key Laboratory of Functional Polymer Materials, Institute of Polymer Chemistry, College of Chemistry and Renewable Energy Conversion and Storage Center (RECAST), Nankai University, Tianjin, 300071, China, liuys@nankai.edu.cn.

[g]Department of Microelectronic Science and Engineering, School of Physical Science and Technology, Ningbo University, Ningbo, 315211, China.

[h]College of New Materials and New Energies, Shenzhen Technology

University, Shenzhen, 518118, China.

Experimental method

Materials

Except as otherwise noted, all materials were used as received without further treated. C60 (99.9%) were purchased from Sigma-Aldrich. Moroxydine Hydrochloride were purchased from Aladdin. Formamidinium iodide (FAI, 99.9%), Methylamine hydrochloride (MACl, 99.9%) and methylammonium iodide (MAI, 99.9%) were purchased from Greatcell Solar Materials (Australia). Cesium iodide (CsI, 99%), lead bromide ($PbBr_2$, 99.99%), Bathocuproine (BCP, 99.9%), Piperazine dihydriodide (PDI, 99.5%) and poly(3,4-ethylenedioxythiophene):poly(styrene sulfonate) (PEDOT:PSS, 1.3-1.7 wt%) were bought from Xi'an Polymer Light Technology Corp. (China). Lead iodide (PbI_2, 99.99%), Gold (Au, 99.999%) and copper (Cu, 99.999%) were purchased from ZhongNuo Advanced Material Technology Co., Ltd (Beijing). PM6, BTP-eC9, and PNDIT-F3N were purchased from Solarmer Materials Inc. *N*, *N*-Dimethylformamide (DMF, 99.8%), dimethyl sulfoxide (DMSO, 99.9%), isopropanol (IPA, 99.5%) and chlorobenzene (CB, 99.8%) were purchased from J&K Chemical. All the solvents were filtered with a 0.22 μm PTFE filter before using.

Preparation of WBG perovskite precursor

The patterned FTO glass substrates were cleaned with a surfactant solution, then soaked in deionized water, acetone, and IPA in the ultrasonic bath for 15 min each. After ultraviolet ozone treatment for 15 min, the substrates were then spin-coated with 4PADCB (0.3 mg/mL in IPA). The SAM films were annealed at 100 C for 10 min. The 1.2 M perovskite ($Cs_{0.25}FA_{0.75}Pb(Br_{0.5}I_{0.5})_3$) precursor solution, which were dissolved in 1 mL mixed solvent of DMF:DMSO (v/v = 4:1). It should be noted that 3.0 mol% of $MAPbCl_3$ was added to the perovskite precursor for device. For the target devices, 0.3 mol% of the

Moroxydine Hydrochloride was added to the perovskite precursor fabrication. For the spin-coating process, the substrate was spun at 4,000 rpm for 45 s with an acceleration of 4,000 rpm/s, and 200 mLof CB was slowly dropped at 15 s before the spin-coating ended. The perovskite films were then annealed at 100 °C for 15 min. Next, 80 μL of PDI (1 mg mL^{-1} in IPA) was dropped on the cooled films at 5000 rpm for 30 s, followed by annealing at 100 °C for 5 min, then annealed at 100 °C for 5 min. Then, 40 nm of C60 and 8 nm of BCP was thermally evaporated under pressure of 4×10^{-5} Torr at the evaporation rate of 0.2 Å s^{-1}. The films were transferred to the thermal evaporator, where 100 nm Cu was deposited to complete the device fabrication.

Perovskite-OSC tandem device fabrication

After completing the deposition of the C60 layer, substrates were transferred to atomic layer deposition (ALD, GEMStar XT, Arradiance) chamber, 20 nm of SnO_2 was deposited on ALD system at around 100 °C. After the ALD deposition, the substrates were covered with a 1.5 nm ultra-thin gold layer through thermal evaporation. Then, 100 μL of PEDOT:PSS solution (diluted with IPA, 1:1 volume ratio) was spin-coated on the WBG substrates, followed by annealing at 100 °C in air for 25 min. The film was transferred to a glovebox where the OSC precursor (D/A = 1:1.2 (w/w), with a PM6 concentration of 8 mg/mL and 0.5% 1,8-diiodooctane [v/v] as an additive in chloroform) was spin-coated at 3,000 rpm for 30 s and annealed at 100 °C for 5 min. Next, PNDIT-F3N was deposited by spin-coating its 1 mg/mL solution in methanol at 3,000 rpm for 30 s. Finally, the film was transferred to the thermal evaporator system to deposit 100 nm Ag as the top electrode to finish the tandem device fabrication process.

Characterizations of perovskite

UV-vis absorption spectra were measured using a spectrophotometer (PerkinElmer Lambda 950). The top-view and cross-section morphology of samples was collected by a field-emission SEM (SU8230, Hitachi). The topography of films was obtained using AFM (Dimension Edge, Bruker) with the

tapping mode. KPFM were performed by Bruker Dimension ICON. XRD patterns were measured with an D8 Advanc ECO X-ray Diffractometer using Cu Kα radiation under operating conditions of 25 kV and 15 mA from 5° to 45°. XPS and UPS were characterized by a photoelectron spectrometer (ESCALAB 250Xi, Thermo Fisher Scientific). Steady-state PL spectra were collected using an FLS980 (Edinburgh Instruments Ltd.), equipped with a Xe lamp. TRPL decay dynamics were measured at 650 nm under 465 nm excitation on the Edinburgh FLS980 fluorimeter. PL mapping was obtained using a Raman microscope (LabRAM HR Evolution, HORIBA). Device performance was characterized by a Keithley 2400 source meter and a solar simulator (Enlitech Solar Simulator SS-F7-3A) which offered the simulated AM1.5 G illumination of 100 mW cm^{-2}. The *J-V* curves were obtained from reverses scan (1.42 V to -0.1 V) and forward scan (-0.1 V to 1.42 V) with a voltage step of 10 m for WBG PSC, The *J-V* curves were obtained from reverses scan (2.23 V to -0.1 V) and forward scan (-0.1 V to 2.23 V) with a voltage step of 20 m for PO-TSC. The transient photovoltaic current (TPC) and transient photovoltage (TPV) was obtained by transient photoelectric streamer voltage measurement system (SouthPort SP-TPVC). EQE was measured by chopped light at 165 Hz under AC mode (QE-R, Enlitech). EIS was measured on a CHI660 electrochemical workstation (CH Instrument Inc.)

Femtosecond (fs) Transient Absorption (TA) Spectroscopy Characterization

For femtosecond transient absorption spectroscopy, the fundamental output from Yb:KGW laser (1030 nm, 220 fs Gaussian fit, 100 kHz, Light Conversion Ltd) was separated to two light beam. One was introduced to NOPA (ORPHEUS-N, Light Conversion Ltd) to produce a certain wavelength for pump beam, the other was focused onto a YAG plate to generate white light continuum as probe beam. The pump and probe overlapped on the sample at a small angle less than 10°. The transmitted probe light from sample was

collected by a linear CCD array.

MMP of wide-bandgap perovskite solar cells

The operational stability tests were carried out at the maximum power point (MPP) for the unencapsulated cells under one-sun illumination in N_2 atmosphere. The illumination was generated using a LED lamp-based solar simulator. The bias at the MPP was calculated and applied automatically. The light intensity was calibrated by a standard silicon reference cell from Newport.

Other characterizations

^{1}HNMR spectra were collected on a Bruker AVANCE III HD 300 MHz spectrometer in DMSO- d6 solution with TMS as a reference. FTIR was characterized by Thermofisher Nicolet iS50.

Supporting Figures

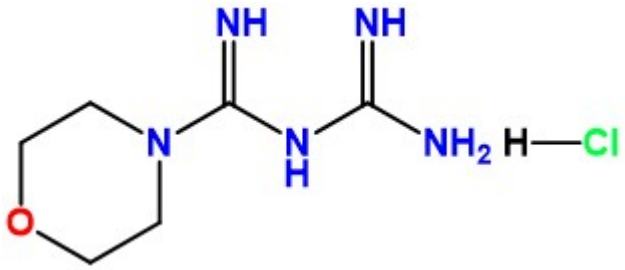

Figure S1. The chemical structures of MODCl molecule.

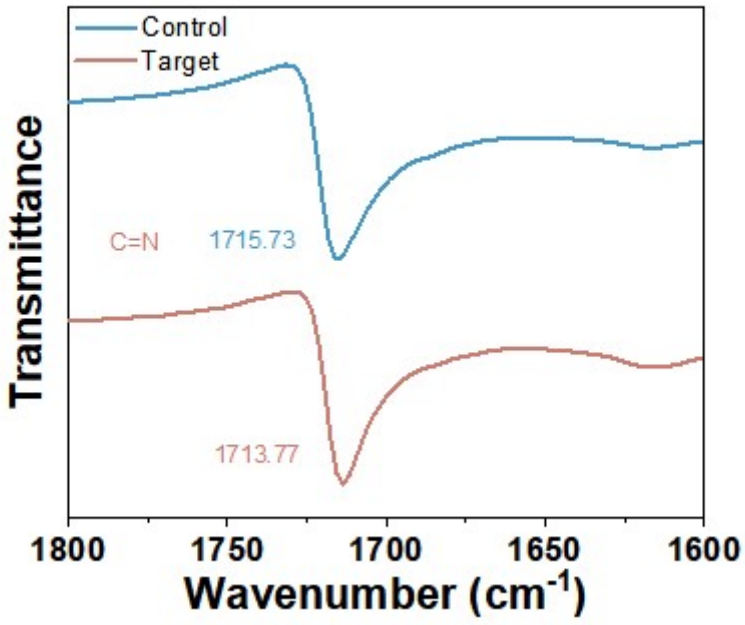

Figure S2. FTIR spectra patterns of Control and target.

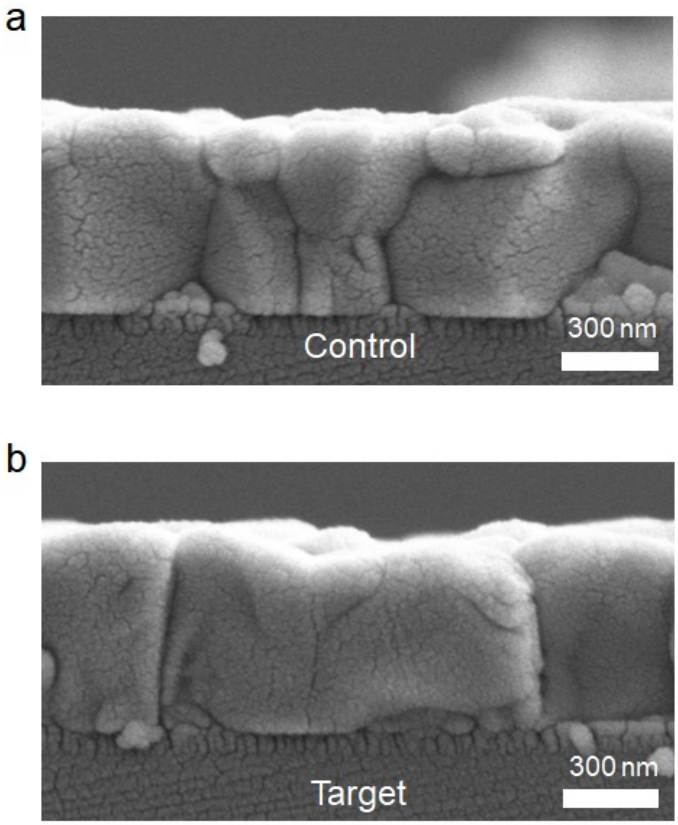

Figure S3. (a) Cross-sectional SEM of the control film. (b) Cross-sectional SEM of the target film.

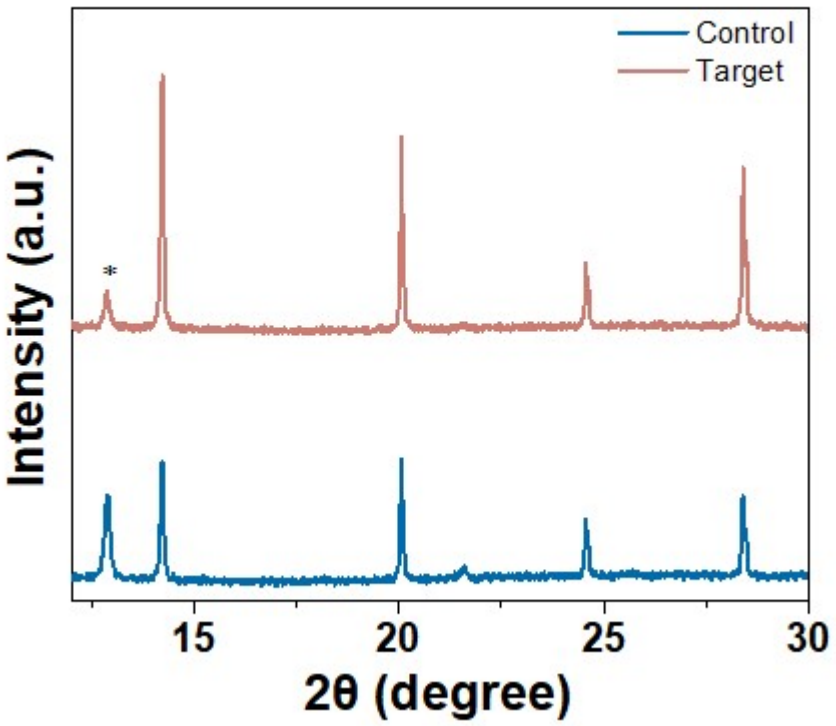

Figure S4. XRD patterns of the control and target perovskite films.

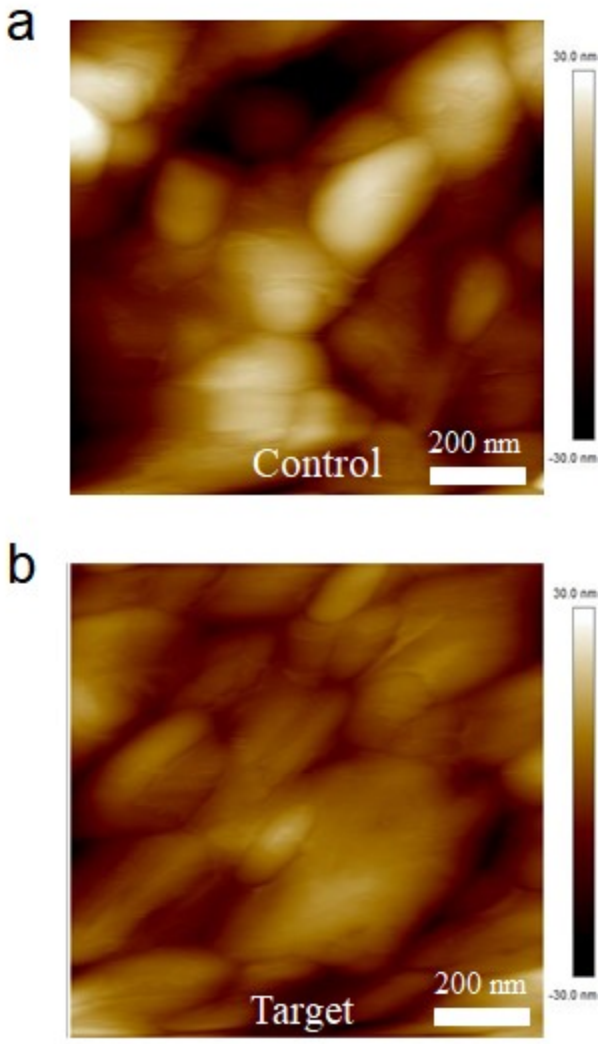

Figure S5. (a) Taping-mode AFM height images of control perovskite films. (b) Taping-mode AFM height images of target perovskite films.

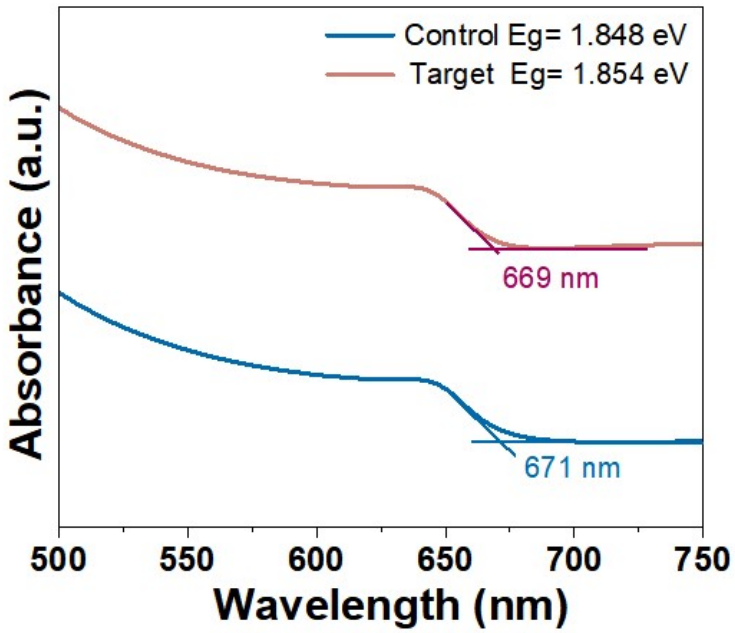

Figure S6. UV absorption spectra of the control and target perovskite films.

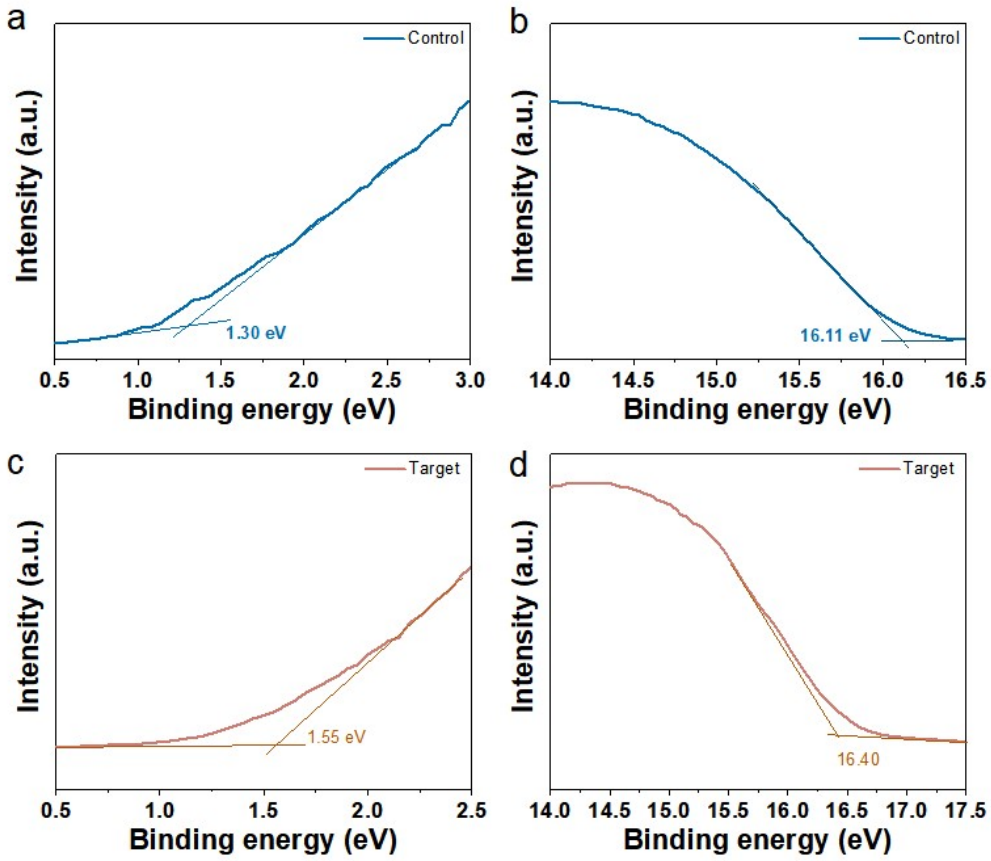

Figure S7. (a) Energy difference between Fermi energy levels and VB for control film. (b) Secondary cutoff region of UPS for control film. (c) Energy difference between Fermi energy levels and VB for control film. (d) Secondary cutoff region of UPS for control film.

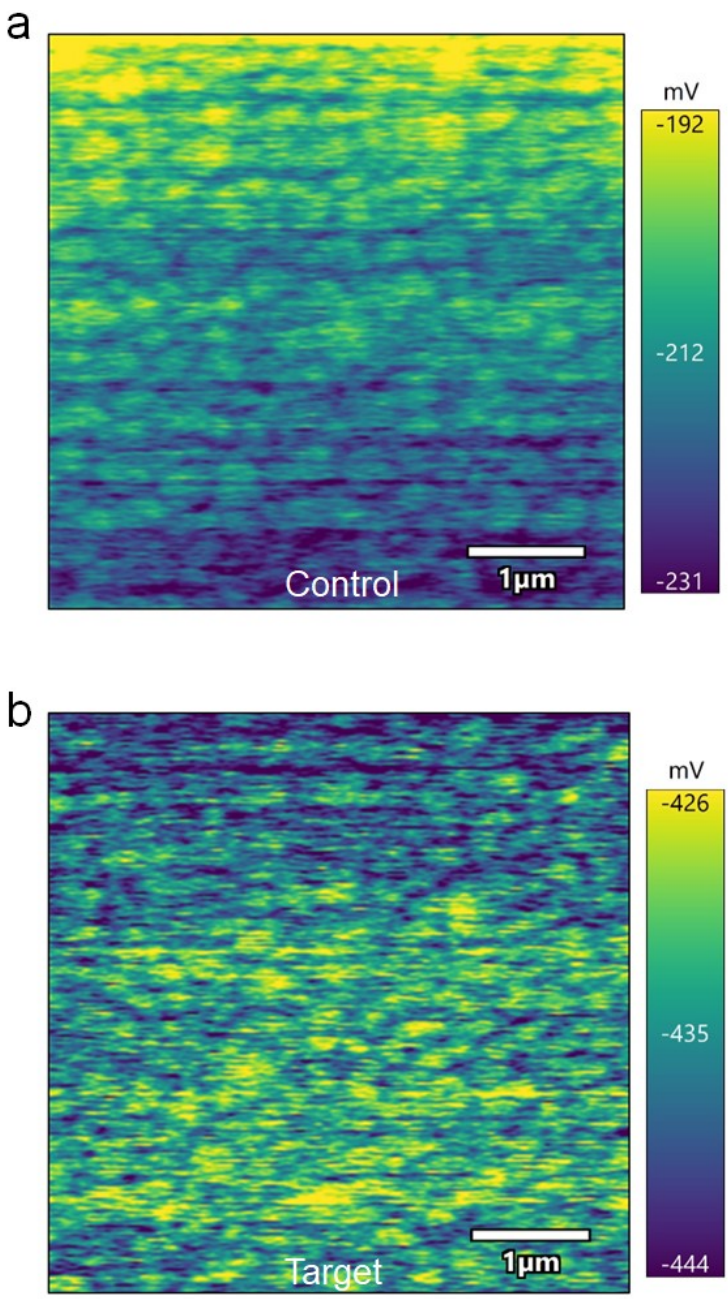

Figure S8. (a) KPFM surface potential images of the control film. (b) KPFM surface potential images of the target film.

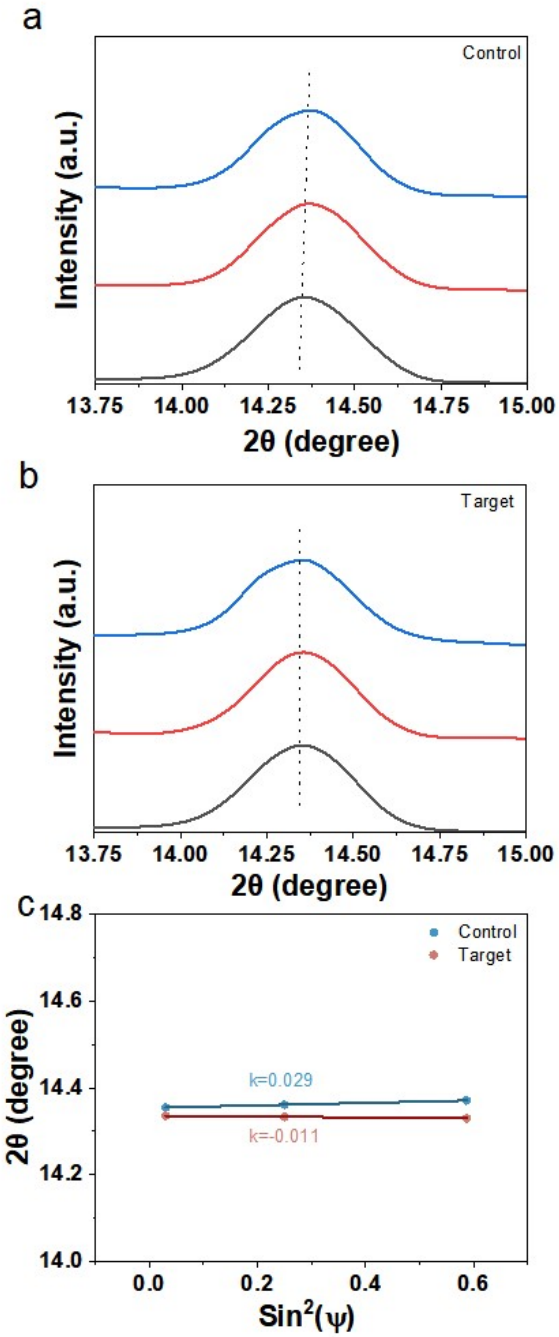

Figure S9. (a) GIXRD of control film with different instrumental ψ values. (b) GIXRD of target film with different instrumental ψ values. (c) Linear fit of 2θ-sin^{2}ψ for control and target film.

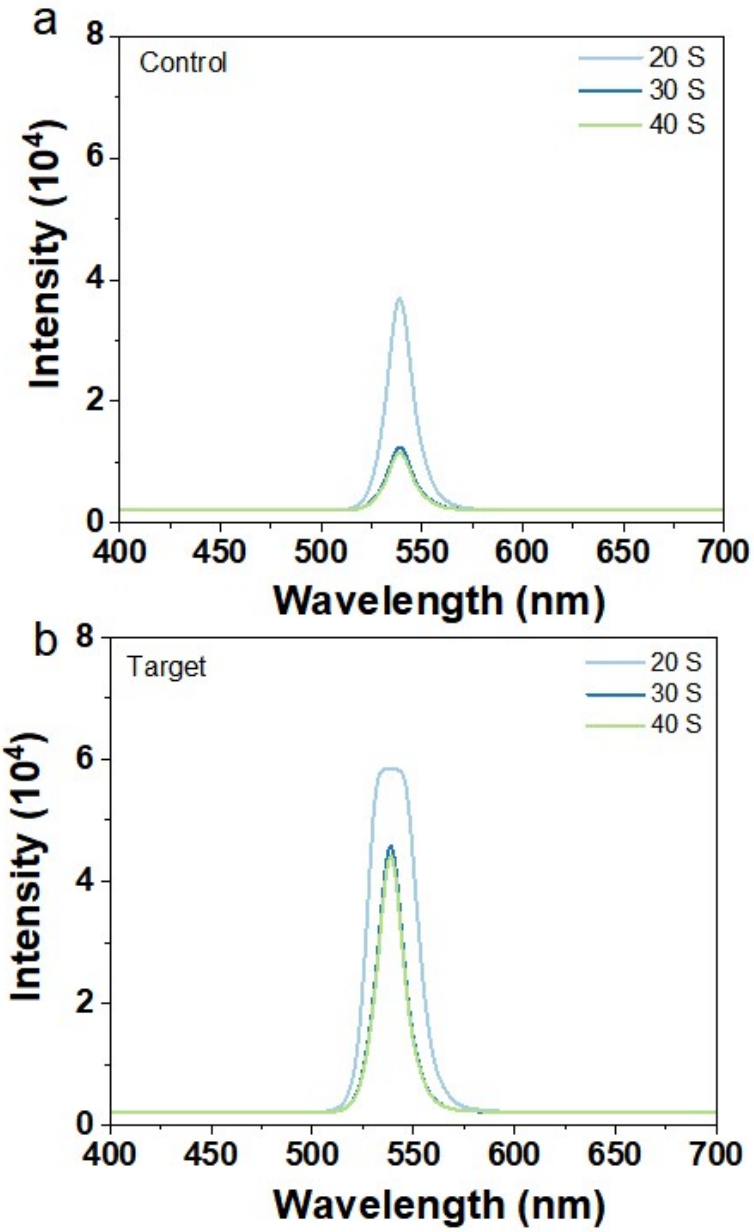

Figure S10. The PL intensity of control and target from Figure 3 (**a**) and (**b**) at 20s, 30s and 40s.

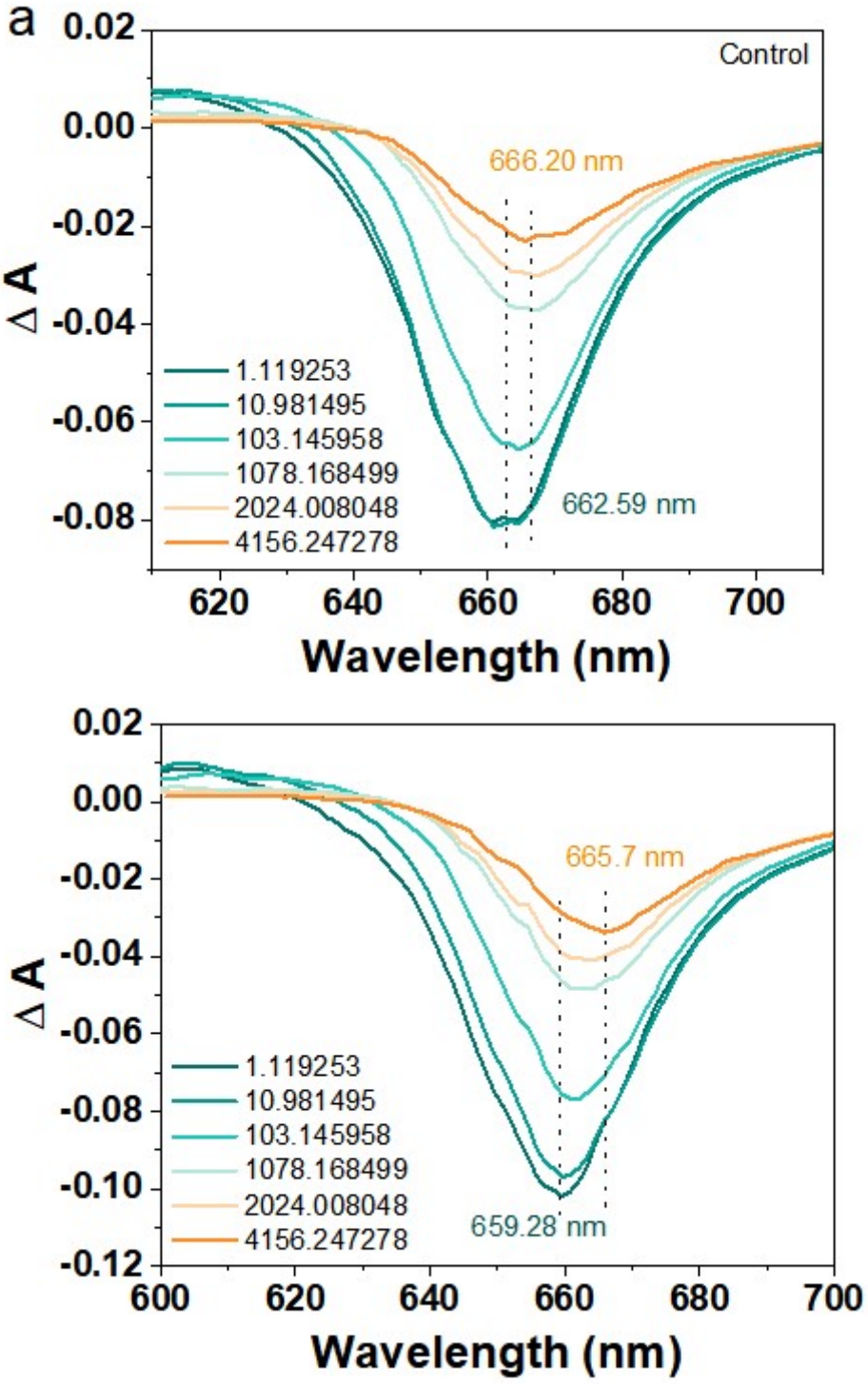

Figure S11. TA spectra at various post-pump delay times of WBG perovskite thin films prepared with the structure FTO/4PADCB/control (**a**) and target (**b**) film. The pump excitation energy is 475 nm incident from the top of the perovskite samples.

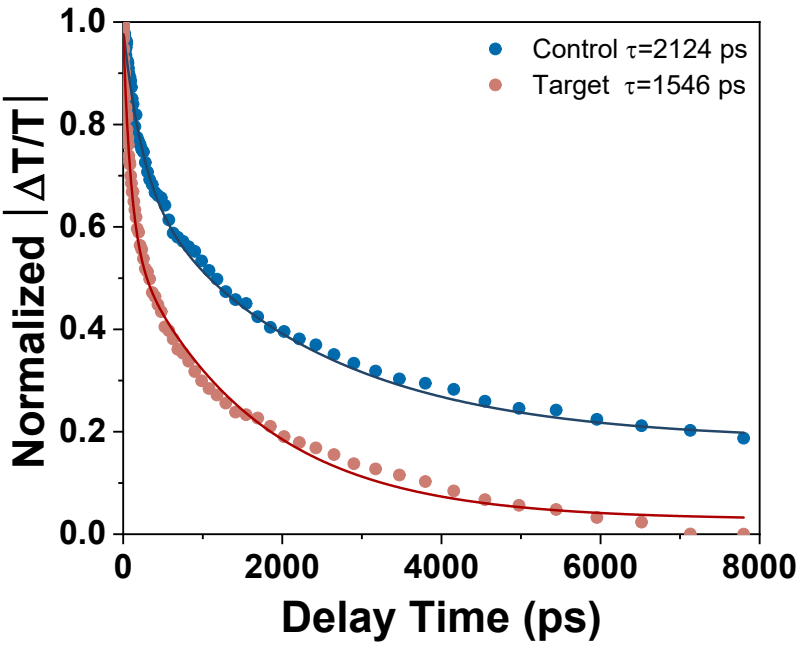

Figure S12. The lifetime of FTO/4PADCB/perovskite films under photo-induced absorption.

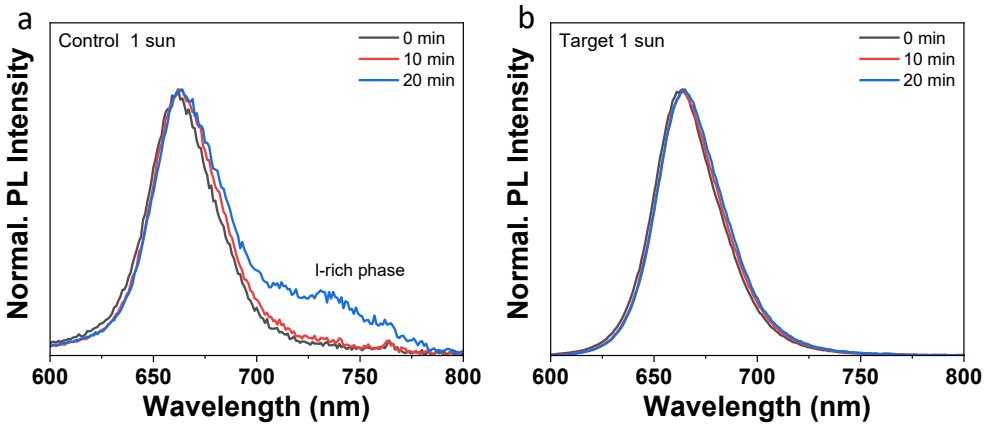

Figure S13. PL evolution of WBG film under 1 sun illumination for 20 min.

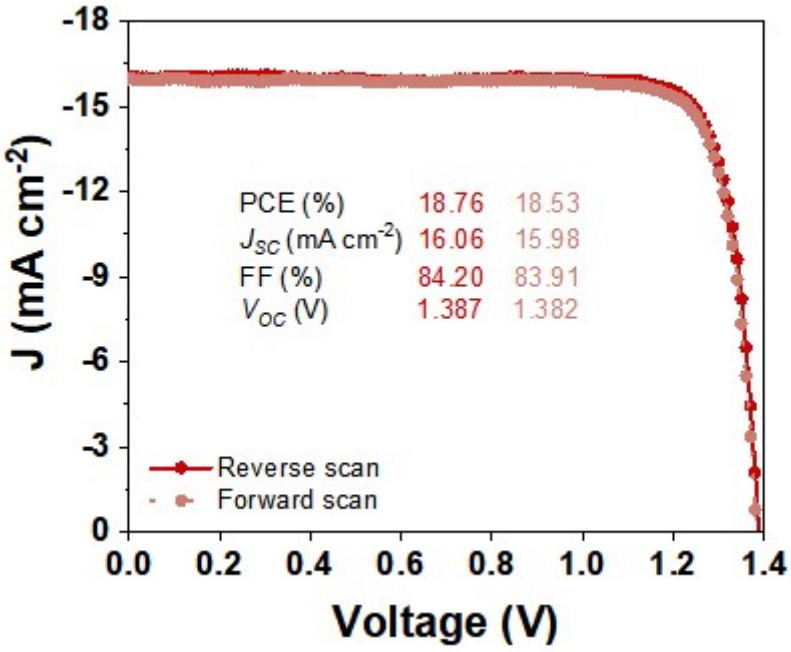

Figure S14. *J–V* characteristics of target device under forward and reverse scans, with corresponding performance parameters are included in the figure.

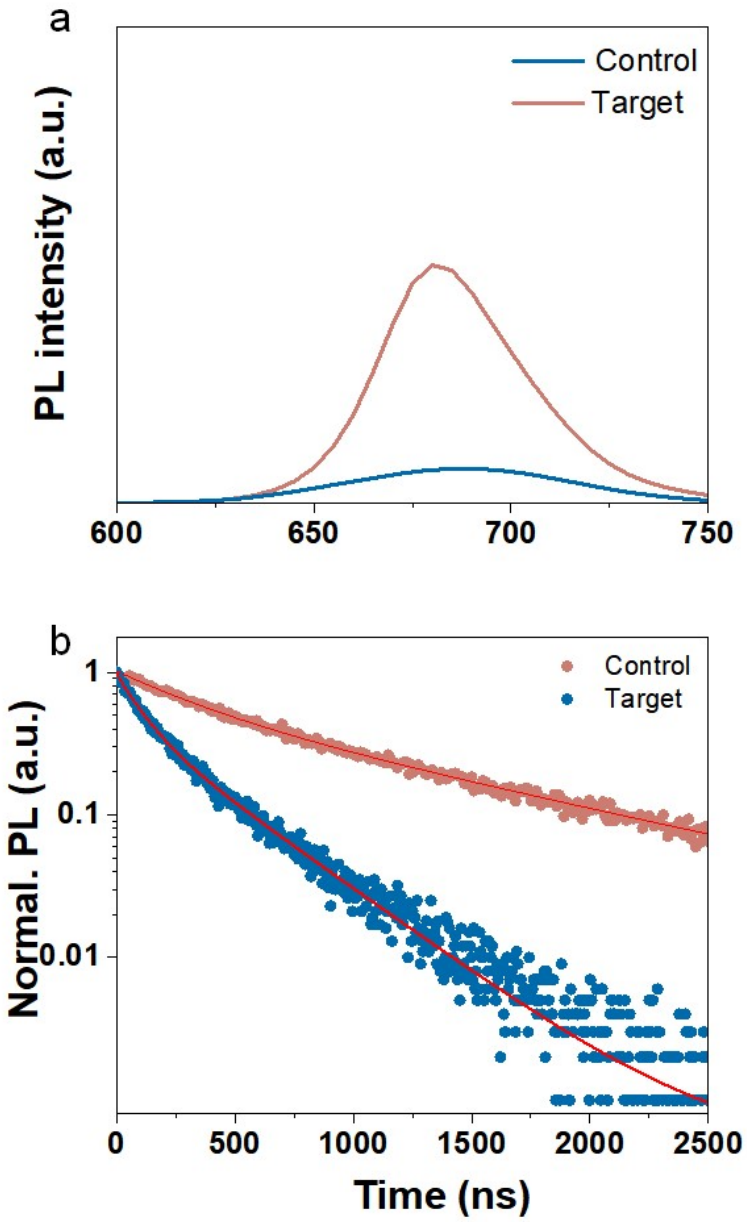

Figure S15. (**a**) PL spectra of control and target WBG perovskite films. (**b**) TRPL spectra of control and target WBG perovskite films.

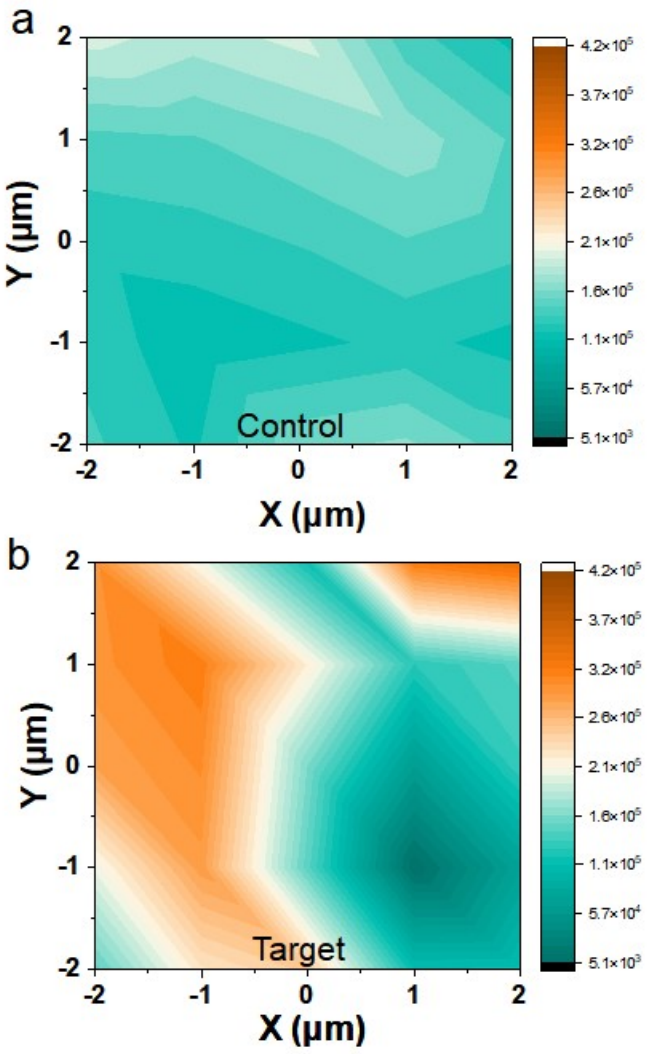

Figure S16. PL mapping of control and target perovskite films.

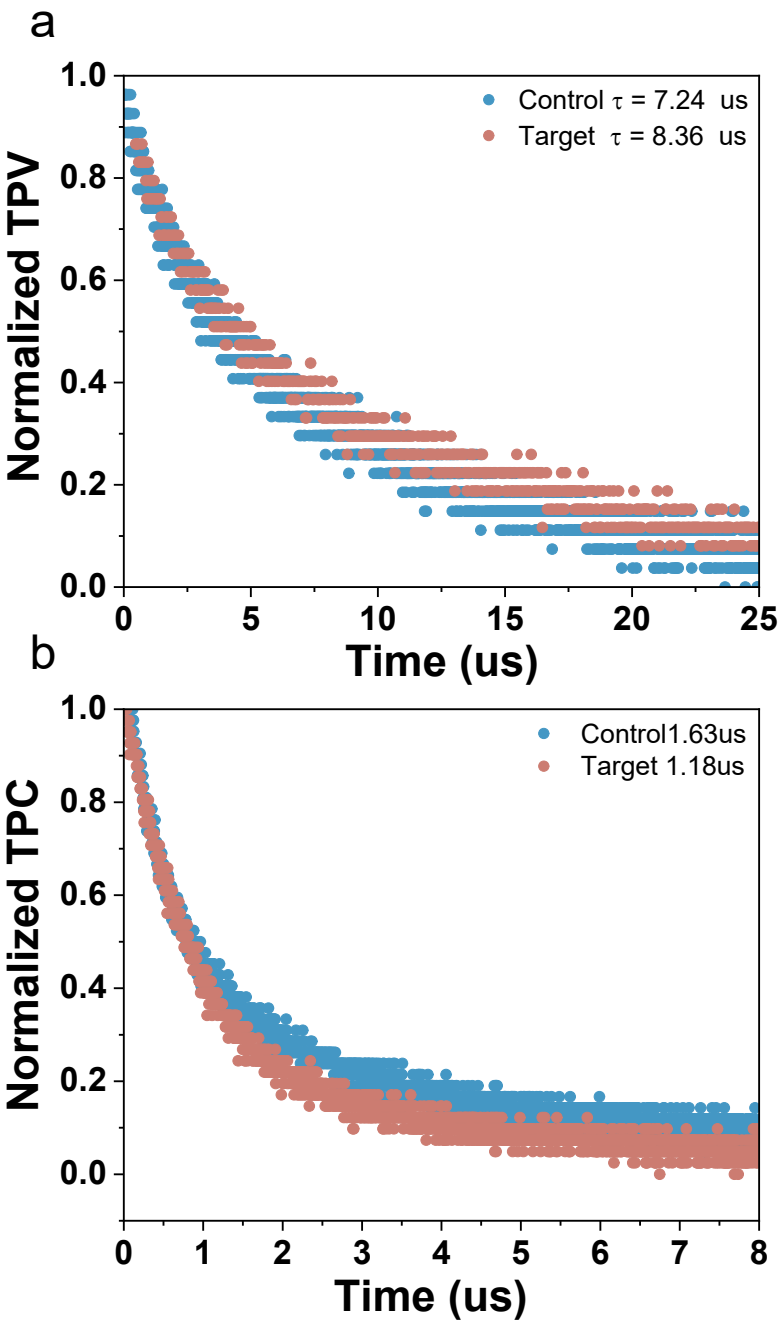

Figure S17. (**a**) Transient photovoltage (TPV) decay curves. (**b**) Transient photocurrent (TPC) decay curves.

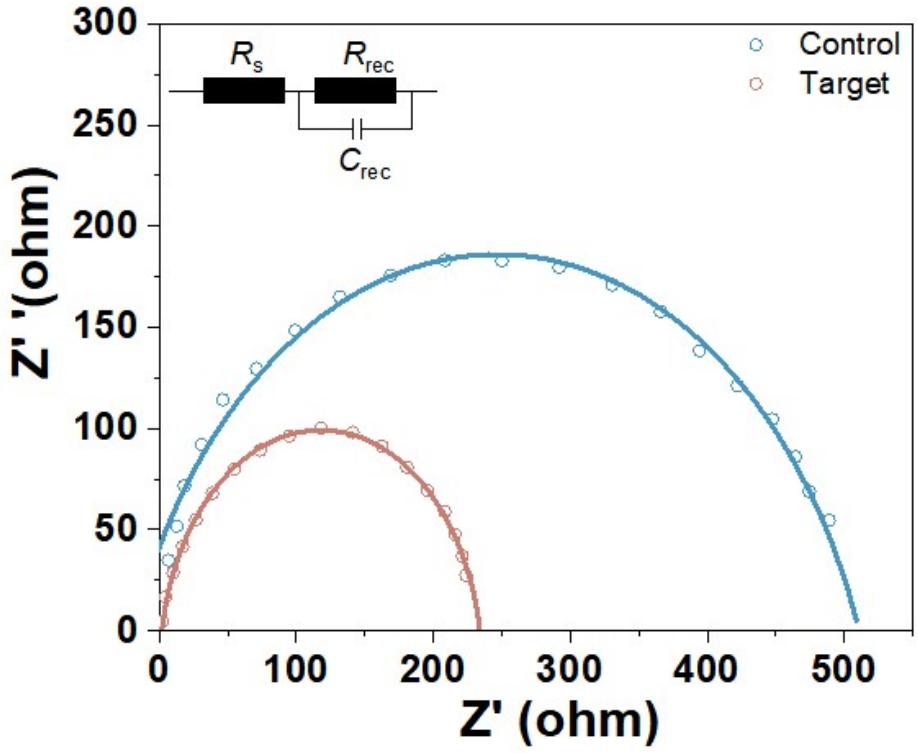

Figure S18. Nyquist plots of control and target PSCs measured in the dark The inset shows the equivalent circuit.

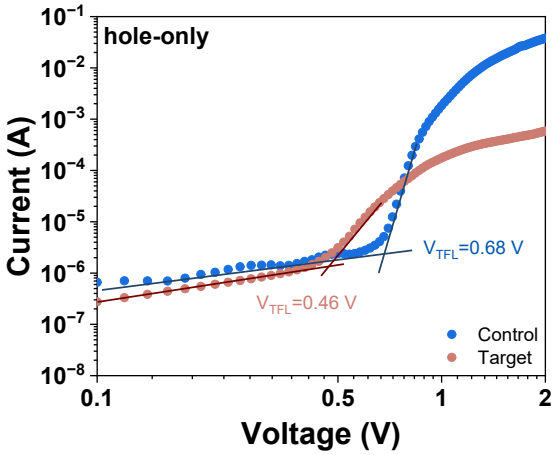

Figure S19. SCLC spectra of the control and target with the structure FTO/4PADCB/PVK/MoOx/Ag.

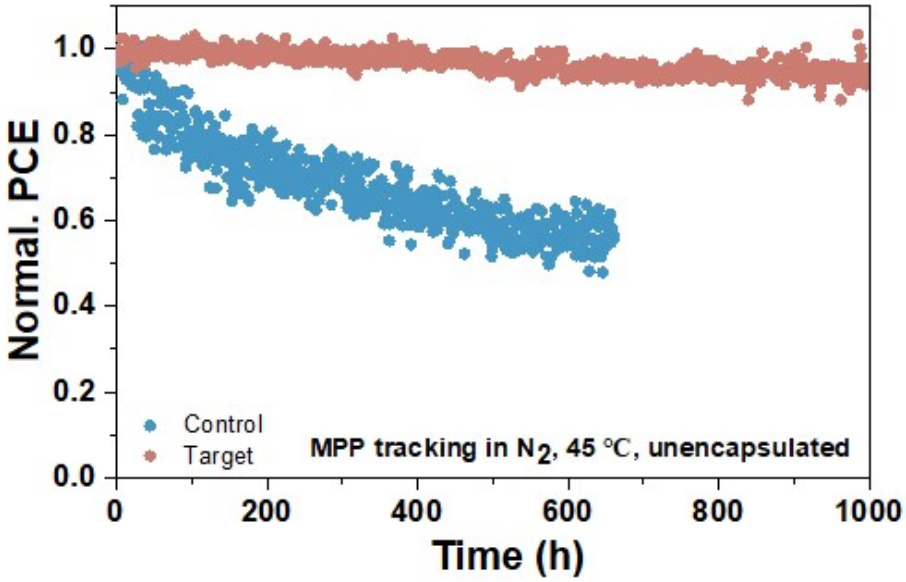

Figure S20. MPP tracking of control and target devices under 1 sun illumination in the N_2 environment.

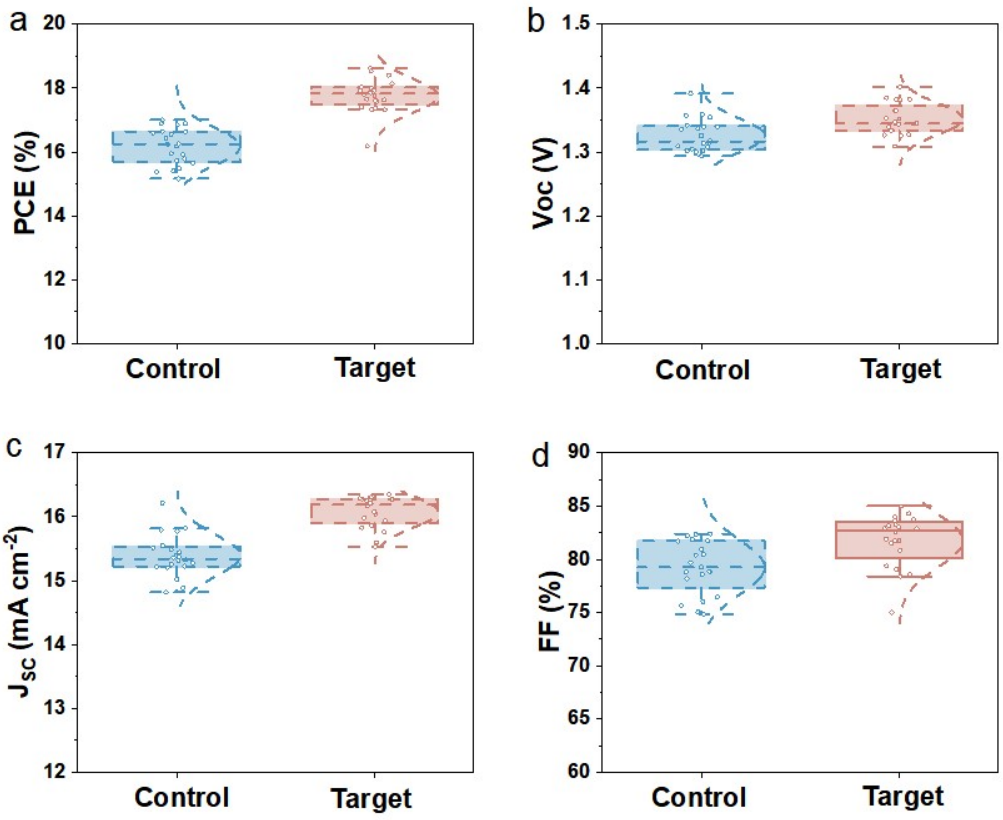

Figure S21. Statistical PCE (a), V_{OC} (b), J_{SC} (c) and FF (d) data of the control and target devices.

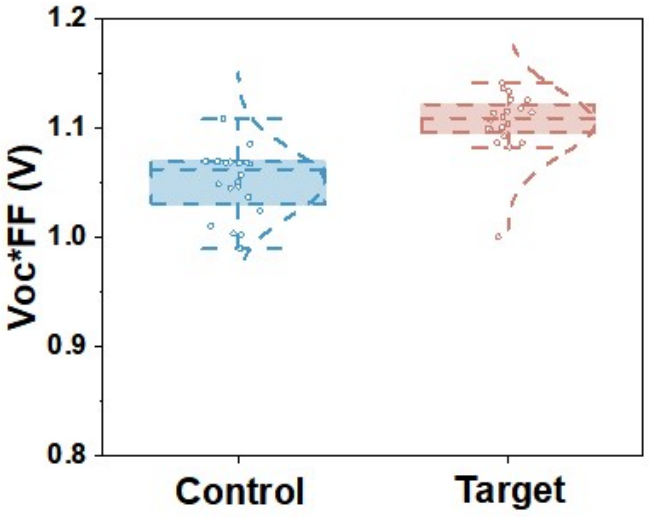

Figure S22. V_{OC}×FF products of control and target PSCs.

Supporting Tables

Table S1 Summary of photovoltaic parameters of target with different concentrations.

	J_{SC}	V_{OC}	FF	PCE
0.1 mol%	16.11	1.362	81.46	17.88
0.3 mol%	16.06	1.387	84.20	18.76
0.5 mol%	15.38	1.400	78.88	16.99

Table S2. Summary of photovoltaic parameters of control and target WBG device.

	J_{SC}[mA cm^{-2}]	V_{OC} [V]	FF [%]	PCE [%]
Control (w/o PI)	15.87	1.313	78.99	16.46
Control (w PI)	16.19	1.353	79.65	17.45
Target	16.06	1.387	84.20	18.76

Table S3. The PL carrier lifetimes extracted from the TRPL decay measurements.

Devices	τ_{ave}(ns)	τ_1(ns)	A_1(%)	τ_2 (ns)	A_2(%)
Control	302.51	102.22	50.88	365.86	46.20
Target	1043.95	336.25	43.81	1195.50	57.54

Table S4. Summary of reports on performance of 1.80-1.89 eV wide-bandgap PSCs.

Eg (eV)	Device Configuration	VOC (V)	J_{SC} ($mAcm^{-2}$)	FF (%)	PCE (%)	Reference
1.80	n-i-p	1.230	19.10	76.00	17.90	Adv. Mater. 31, 1904494 (2019).
1.8	p-i-n	1.263	17.4	79.7	17.7	Adv. Mater. 34, 2110356(2022).
1.8	p-i-n	1.22	17	78	16.3	Nat. Commun. 10, 4498(2019).
1.8	p-i-n	1.26	18.07	83.44	18.92	Nano Energy 114, 108653(2023).
1.8	p-i-n	1.25	17.2	79.07	17	Adv. Mater. 35, 2211742(2023).
1.8	p-i-n	1.27	16.2	82.3	16.94	Nat. Commun. 14, 932 (2023).
1.8	p-i-n	1.34	17.9	83.6	20.1	Science 382, 284-289 (2023).
1.8	p-i-n	1.34	18.2	83.9	20.3	Adv. Mater. 36, 2307743(2024).
1.8	n-i-p	1.285	17.52	81.35	18.31	Energy Environ. Sci.17,1046-1060 (2024).
1.81	p-i-n	1.21	17.78	79.5	17.1	Small 16, 1907226 (2020).
1.82	p-i-n	1.25	16.9	83	17.6	Adv. Mater. 34, 2108829(2022).
1.82	p-i-n	1.26	15.6	77.5	15.2	Sci. Adv. 5, eaav8925 (2019).
1.82	p-i-n	1.2	14.55	82.32	14.35	Adv. Energy Mater. 10,1903085 (2020).
1.82	p-i-n	1.32	16.98	83.33	18.69	Advanced Materials, n/a, 2411027.
1.83	p-i-n	1.3	14	67	12.2	Nano Lett. 18, 3985-3993(2018).
1.83	n-i-p	1.09	17.9	66.1	12.91	J. Am. Chem. Soc. 141, 2684-2694 (2019).
1.83	p-i-n	1.15	14.68	73	12.29	Adv. Energy Mater. 8,1801954 (2018).
1.84	n-i-p	1.12	16.36	76.87	14.08	J. Mater. Chem. A 7, 18488(2019).
1.85	p-i-n	1.34	15.6	81	16.8	Nature 604, 280-286 (2022).
1.85	p-i-n	1.36	16.21	83.21	18.14	Adv. Mater. 36, 2306568(2024).
1.85	p-i-n	1.35	16.78	83.29	18.87	Adv. Mater. 35, 2305946(2023).
1.85	p-i-n	1.387	16.06	84.20	18.78	This work
1.86	n-i-p	1.42	14.39	82	16.72	Adv. Funct. Mater. 32,2207554 (2022).
1.86	p-i-n	1.22	17.65	73	15.7	Surf. Interfaces 37, 102680(2023).
1.86	n-i-p	1.28	14	78.2	14	Nat. Commun. 10, 4686(2019).
1.86	n-i-p	1.25	15.33	76.3	14.63	Nanoscale 11, 14553-14560(2019).
1.86	p-i-n	1.223	16.35	79.62	15.92	Nano-Micro Lett. 12, 170(2020).
1.86	p-i-n	1.366	16.1	84.2	18.52	*Joule* **2024**, 8, 2554.
1.87	p-i-n	1.21	13.42	81.36	13.16	Adv. Energy Mater. 10,1903085 (2020).
1.87	n-i-p	1.26	17.16	80.14	17.37	Sci. Bull. 64, 1743-1746(2019).
1.87	n-i-p	1.23	17.04	76.49	15.98	Sci. Bull. 64, 507-510 (2019).
1.88	n-i-p	1.31	15.81	82.88	17.16	Adv. Funct. Mater. 33,2212599 (2023).
1.88	n-i-p	1.18	15.8	72.7	13.6	Adv. Energy Mater. 9,1900896 (2019).
1.88	p-i-n	1.36	16.1	83.8	18.4	Nature 2024.DOI:10.1038/s41586-024-08160-y
1.89	n-i-p	1.15	16.82	75.73	14.69	Joule 3, 2485-2502 (2019).

1.89	p-i-n	1.28	15	77	14.8	ACS Appl. Mater. Interfaces11, 43303-43311 (2019).
1.89	p-i-n	1.2	14.22	82.68	14.11	J. Phys. Chem. Lett. 10, 6382-6388 (2019).
1.89	n-i-p	1.45	14.52	79.21	16.7	ACS Energy Lett. 7, 4071-4080 (2022)

Table S5 Summary of photovoltaic parameters of WBG device with E_g=1.80 eV.

E_g	Device	J_{sc}	V_{oc}	FF	PCE
1.80 eV	Control	17.47	1.328	79.66	18.48
	Target	17.12	1.354	83.86	19.43

Table S6. Summary of photovoltaic parameters of WBG, OSC and TSC device.

	J_{SC}[mA cm^{-2}]	V_{OC} [V]	FF [%]	PCE [%]
WBG	16.06	1.387	84.20	18.76
OSC	27.93	0.852	78.02	18.58
TSC	14.56	2.210	80.56	25.98

Table S7. Summary of reports on performance of PO-TSC.

	PCE (%)	**V_{OC} (V)**
1[1]	24	2.15
2[2]	24.07	2.09
3[3]	25.22	2.151
4[4]	25.13	2.144
5[5]	25.56	2.126
6[6]	26.4	2.16
7[7]	25.54	2.15
8[8]	25.92	2.135
This work	25.98	2.210

REFERENCES

[1] K. O. Brinkmann, T. Becker, F. Zimmermann, C. Kreusel, T. Gahlmann, M. Theisen, T. Haeger, S. Olthof, C. Tückmantel, M. Günster, T. Maschwitz, F. Göbelsmann, C. Koch, D. Hertel, P. Caprioglio, F. Peña-Camargo, L. Perdigón-Toro, A. Al-Ashouri, L. Merten, A. Hinderhofer, L. Gomell, S. Zhang, F. Schreiber, S. Albrecht, K. Meerholz, D. Neher, M. Stolterfoht, T. Riedl, *Nature* **2022**, 604, 280.

[2] Z. Ma, Y. Dong, R. Wang, Z. Xu, M. Li, Z. a. Tan, *Adv. Mater.* **2023**, 35, 2307502.

[3] S. Wu, Y. Yan, J. Yin, K. Jiang, F. Li, Z. Zeng, S.-W. Tsang, A. K. Y. Jen, *Nat. Energy* **2024**, 9, 411.

[4] X. Guo, Z. Jia, S. Liu, R. Guo, F. Jiang, Y. Shi, Z. Dong, R. Luo, Y.-D. Wang, Z. Shi, J. Li, J. Chen, L. K. Lee, P. Müller-Buschbaum, D. S. Ginger, D. J. Paterson, Y. Hou, *Joule* **2024**, 8, 2554.

[5] X. Wu, D. Zhang, B. Liu, Y. Wang, X. Wang, Q. Liu, D. Gao, N. Wang, B. Li, L. Wang, Z. Yu, X. Li, S. Xiao, N. Li, M. Stolterfoht, Y.-H. Lin, S. Yang, X. C. Zeng, Z. Zhu, *Adv. Mater.*, n/a, 2410692.

[6] X. Jiang, S. Qin, L. Meng, G. He, J. Zhang, Y. Wang, Y. Zhu, T. Zou, Y. Gong, Z. Chen, G. Sun, M. Liu, X. Li, F. Lang, Y. Li, *Nature* **2024**.

[7] M. Chen, Y. Li, Z. Zeng, M. Liu, T. Du, X. Huang, L. Bi, J. Wang, W. Jiang, Y. An, S.-W. Tsang, J. Yin, S. Wu, A. K. Y. Jen, *Energy Environ. Sci.* **2024**.

[8] S. Kang, Z. Wang, W. Chen, Z. Zhang, J. Cao, J. Zheng, X. Jiang, J. Xu, J. Yuan, J. Zhu, H. Chen, X. Chen, Y. Li, Y. Li, *Adv. Mater.*, n/a, 2411027.